

High Resolution Imaging of the Medial Temporal Lobe in Alzheimer's Disease and Dementia with Lewy Bodies

Michael J. Firbank^{a,*}, Andrew M. Blamire^b, Andrew Teodorczuk^a, Emma Teper^a, Emma J. Burton^a, Dipayan Mitra^c and John T. O'Brien^a

^a*Institute for Ageing and Health, Newcastle University, Newcastle, UK*

^b*Newcastle MR Centre, Newcastle University, Newcastle, UK*

^c*Department of Neuroradiology, Newcastle General Hospital, Newcastle, UK*

Handling Associate Editor: Marco Bozzali

Accepted 13 May 2010

Abstract. We used high resolution (0.3 mm in-plane) coronal 3T magnetic resonance (MR) imaging of the medial temporal lobe in 16 subjects with Alzheimer's disease (AD), 16 with dementia with Lewy bodies (DLB), and 16 similarly aged healthy subjects. On the anterior section of the hippocampus body, regions of interest were manually drawn blind to diagnosis on the CA1, CA2, and CA3/4 subregions, and the width of the subiculum and entorhinal cortex was measured. Controlling for intracranial volume, age, and years of education, we found the subiculum thickness was significantly reduced in AD (2.03 ± 0.29 mm) compared to both control (2.37 ± 0.28 mm, $p = 0.008$) and DLB (2.35 ± 0.24 mm, $p = 0.001$) subjects. The area of CA1 was likewise reduced in AD compared to controls and DLB. In the hippocampus images, a hypointense line is visible between CA1 and CA3/4. This line was significantly less distinct in AD, suggesting disease related changes to this region. Future studies should investigate whether subiculum thickness or the hypointense line could be a diagnostic feature to help discriminate AD from DLB.

Keywords: Alzheimer's disease, dementia with Lewy bodies, hippocampus, MRI, subiculum

INTRODUCTION

Alzheimer's disease (AD) is characterized by extensive tissue loss in the medial temporal lobe region, especially in the hippocampus and entorhinal cortex. However, the hippocampus has a complex anatomical structure, and is not uniformly affected in disease. A number of MRI studies using T1 weighted imaging, and approximately isotropic 1 mm^3 voxels, have shown

that, along with the entorhinal cortex, atrophy in AD is largely confined to the CA1 and subiculum regions of the hippocampus [1,2], consistent with the major site of pathology observed at autopsy [3]. However, these studies have not directly visualized subfields but relied on inferring the location of the subregions from the known anatomy of the hippocampus surface. Using a high in plane resolution coronal T2 weighted sequence at 4T, Mueller and colleagues have shown it is possible to differentiate the hippocampal subregions directly in both control [4] and AD [5].

Previous MR imaging studies in dementia with Lewy bodies (DLB) have shown that the degree of hippocampal atrophy is less in DLB than in AD [6–8]. Using shape analysis on hippocampi manually traced from

*Correspondence to: Michael J. Firbank, Institute for Ageing and Health, Newcastle University, Wolfson Research Center, Campus for Ageing and Vitality, Newcastle upon Tyne NE4 5PL, UK. Tel.: +44 (0)191 248 1319; Fax: +44 (0)191 248 1301; E-mail: m.j.firbank@ncl.ac.uk.

T1 weighted images, a study [9] also found less atrophy in DLB compared to AD. The distribution of atrophy was somewhat different, affecting more anterior regions in DLB and posterior regions in AD, consistent with more CA2 and CA3 atrophy in DLB. Kenny and colleagues [10] measured the entorhinal cortex using a region of interest on T1 weighted images and found comparable atrophy in AD and DLB. Neuropathological studies have found Lewy bodies neurites preferentially in the CA2 and CA3 region [11,12], though Harding [13] found no difference between control and DLB in any hippocampal subregion volume.

The purpose of this study was to investigate atrophy of the subfields of the anterior part of the body of the hippocampus, using high resolution coronal imaging of the medial temporal lobe. We hypothesised that there would be more atrophy of the CA1 and subiculum in AD, with more atrophy of the CA2 or CA3/4 region in DLB and that these changes may be helpful for differentiating AD from DLB.

MATERIALS AND METHODS

Subjects

We recruited 16 people with AD and 16 with DLB from clinical Old Age Psychiatry, Geriatric Medicine and Neurology Services. Sixteen healthy subjects of similar age were also recruited.

All subjects were aged over 60 and did not have contra-indications for MRI. Subjects with dementia had mild to moderate severity (MMSE > 10). All AD subjects fulfilled criteria for probable AD according to NINCDS/ADRDA [14]. DLB cases similarly met criteria for probable DLB according to the consensus criteria [15] (i.e., they met two or more of the core features of fluctuating cognition, visual hallucinations, and parkinsonism). Nine of the DLB subjects had a ^{123}I -FP-CIT SPECT scan, all of whom demonstrated reduced dopamine transporter uptake in the basal ganglia. All diagnoses were made by consensus between two experienced clinicians, a method we have previously validated against autopsy diagnosis [16]. Diagnoses were made independent of MRI scanning. Routine clinical workup for dementia included detailed physical, neurological, and neuropsychiatric examinations, including screening blood tests and CT scan. Presence of diabetes and hypertension were determined through a combination of medical records, interview with subject, and examining medications. Additional assess-

ments performed were of cognition (Cambridge Cognitive Examination (CAMCOG)) [17], mood (Cornell depression scale) [18], neuropsychiatric features (Neuropsychiatric inventory (NPI)) [19], clinical fluctuation (Clinical Assessment of Fluctuation scale) [20], memory (Rey auditory verbal learning test [21]), and motor features of parkinsonism (UPDRS subsection III) [22].

Exclusion criteria included severe concurrent illness (apart from dementia for patients), space occupying lesions on imaging, history of stroke, and contraindications to MRI. In addition, controls had no history of psychiatric illnesses.

The study was approved by the local ethics committee, and all subjects gave signed informed consent for participation.

MRI acquisition

Subjects were scanned on a 3T MRI system (Intera Achieva scanner; Philips, Eindhoven, the Netherlands). Images acquired included a T1 weighted volumetric sequence covering the whole brain (MPRAGE, sagittal acquisition, slice thickness 1.2 mm, voxel size 1.15×1.15 mm; TR = 9.6 ms; TE 4.6 ms; flip angle = 8° ; SENSE factor = 2).

We used a high resolution T2 weighted turbo spin echo coronal imaging sequence based on previous work at 4T [4]. Prior to commencing the study, we attempted to optimize the high resolution sequence using a range of TR (2500–5000 ms) and TE (19–80 ms) on a 42 year old volunteer. On the first 13 subjects we used the following sequence: turbo factor 15; 24 slices; slice thickness 2 mm, field of view 210×167 ; pixel resolution 0.41×0.52 mm; TR 2568 ms; TE 19 ms; flip angle 90° . This scan was repeated to collect 2 datasets – acquisition time = $2 \times 2:50$.

After the first 13 subjects (5 Control, 7 AD, 1 DLB), one of the high resolution acquisitions was replaced (see results for explanation of reasons) by 3 acquisitions of a sequence with the following parameters altered (12 slices; pixel resolution 0.27×0.35 mm; TR 3852ms; 3 acquisitions – acquisition time = $3 \times 2:07$). The number of acquisitions was increased to maintain SNR in the face of smaller voxels. The first 13 subjects were not rescanned with the new sequence. Data were acquired using multiple acquisitions to allow correction of patient motion prior to averaging to increase signal to noise ratio. This approach was found to maintain highest resolution in pilot studies compared with direct averaging by the scanner. The coronal images were positioned for each subject so they were angled per-

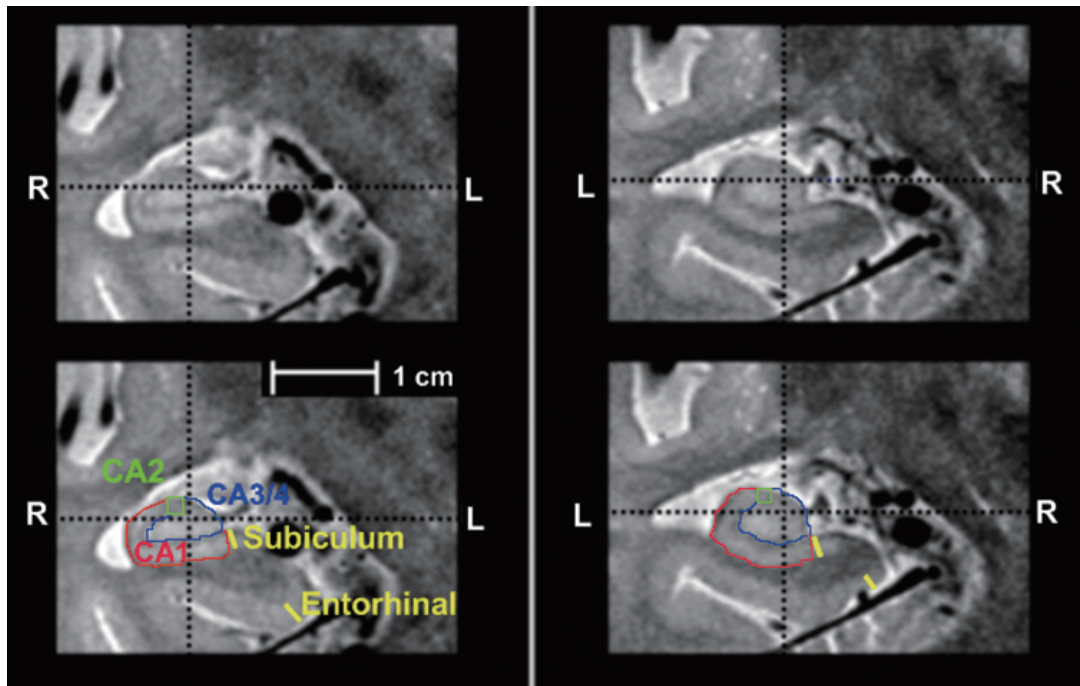


Fig. 1. Close up of hippocampi from one subject in the high resolution T2 weighted coronal sequence. (The left hippocampus has been flipped left-right so that the hippocampus has the same relative orientation). Bottom image shows the regions drawn CA1 (red) CA3/4 (blue), and CA2 (green). The thickness measurement of entorhinal cortex and subiculum is shown as a yellow line. (For reference to color, see the online version of the image). *R* = right, *L* = left.

pendicular to the main axis of the hippocampus. This was achieved by angling the image plane at 25° relative to a line joining the inferior aspect of the genu and splenium of the corpus callosum. This line is similarly oriented to the standard anterior-posterior commissure orientation. We have previously found this to be a reliable and repeatable method to give a good angulation in the temporal lobe.

MRI processing

We used the FLIRT image registration tool [23] (part of FSL; <http://www.fmrib.ox.ac.uk/fsl/>) to register all the high resolution images from each subject together, and interpolate with linear interpolation to 0.27×0.27 mm resolution. A higher signal to noise ratio image was then created by summing together all the registered high resolution images. For the initial 13 subjects for whom two datasets were collected, these datasets were averaged together. For the subsequent subjects for whom four datasets were collected, an image was produced by averaging all four images (three images with 0.27×0.35 mm resolution and one with 0.41×0.52 mm) together. This was found by visual inspection to optimize contrast to noise.

Regions of interest (ROI) were manually drawn on coronal T2 weighted images of the hippocampus sub-regions CA1, CA2, and CA3/4 according to the method of Mueller [4] starting on the slice on which the head of the hippocampus was no longer visible, and the 2 slices posterior to that. This method uses the hypointense line visible on the coronal T2 weighted images in the hippocampus to determine the boundary between CA1 and CA3/4 (Fig. 1). All regions were drawn with the temporal lobe presented with its medial aspect on the right of the screen. Figure 1 depicts the regions. The external boundary of CA1 was drawn starting with a line perpendicular to the subiculum cortex surface where it meets the CA3/4 region, and following the boundary of the hippocampus round to the CA2 region. The hypointense line was used to differentiate CA3/4 from CA1, and from the inferior portion of CA2. The fimbria was excluded. The medial border of CA2 was positioned halfway laterally across the hippocampus, measured from the superficial hippocampal sulcus. CA2 was then drawn as a square angled according to the superior surface of the hippocampus, whose height was determined by the distance between the hypointense line and the superior surface. We calculated the area of each ROI and then averaged val-

Table 1

Reliability measures of hippocampal area/thickness, performed on 6 subjects (12 medial temporal lobes). Final column is agreement between the image with resolution 0.41×0.52 mm and the average of four images (3 with resolution 0.27×0.36 mm and 1 with 0.41×0.52 mm), and these data are from the 4/6 of the subjects who had both sequences. Percent difference is absolute difference in area as percentage of average area, and percent overlap is area in common as a percentage of average area. Values are mean (95% Confidence interval)

	Within observer comparison			Between observer comparison			Initial versus final sequence comparison		
	Percent Difference	Percent Overlap	ICC	Percent Difference	Percent Overlap	ICC	Percent Difference	Percent Overlap	ICC
CA1	7.7 (5–10)	90 (88–91)	0.98	16 (9–23)	76 (72–79)	0.91	5.2 (2–8)	81 (76–86)	0.98
CA2	24 (15–32)	68 (62–75)	0.62	20 (10–29)	34 (25–46)	0.23	20 (11–29)	59 (48–70)	0.20
CA3/4	7.3 (3–11)	90 (88–91)	0.95	22 (15–29)	79 (76–82)	0.80	13 (7–19)	84 (80–88)	0.74
Thicknesses:									
Entorhinal	13.2 (7–20)		0.72	11 (5–16)		0.78	13 (10–15)		0.68
Subiculum	8.0 (4–12)		0.84	11 (7–15)		0.78	10 (7–13)		0.90
CA2	7.0 (4–10)		0.74	19 (11–26)		0.57	12 (9–14)		0.72
Clarity			0.97			0.80			0.58

ICC = intraclass correlation coefficient.

ues over the three slices on which they were defined to give an average area for each structure. An average hippocampus area was defined by summing together the values for CA1, CA2, and CA3/4. All regions were drawn using the freely available itk-snap package [24] (<http://www.itksnap.org/pmwiki/pmwiki.php>) by the same operator (MJF), blinded to diagnosis. Images were displayed with linear interpolation, and image display settings were determined by viewing the image intensity histogram – window levels were set from the width of the main bell-shaped histogram curve at approximately 10% of its height. This display setting enhanced the grey/white matter contrast.

Since the length of the subiculum and entorhinal cortex varied, and because it is known that thickness rather than area measurements are more consistent in these structures [25], we measured the thickness, rather than area, of the subiculum and entorhinal cortex. The imageJ (<http://rsb.info.nih.gov/ij/index.html>) image viewing package was used for distance measurement. This was performed by determining the length of a manually drawn line on the coronal images on three adjacent slices, and calculating the average length. The orientation of the line was drawn (by eye) perpendicular to the surface at the point of measurement. The subiculum thickness was measured on the same three slices as the CA1 region, where the medial border of the hippocampus joined the subiculum (Fig. 1). The entorhinal cortex thickness was measured on the starting slice of the CA1 measurement, and the two anterior slices. Position of entorhinal thickness measurement is also shown in Fig. 1. We also measured the thickness of the CA2 region on the same three slices as the region of interest was drawn, as a potentially more reliable measurement. Since we had no hypothesis regarding laterality, we averaged all left and right measurements.

Reliability was assessed by repeating the region drawing and distance measurement on 6 subjects (= 12 hippocampi) chosen at random (2 control, 2 AD, and 2 DLB) at least a month after initial region drawing. From these, we calculated intraclass correlation coefficient (ICC), percent difference, and (for region measurements) percent overlap. These were defined as
 Percent difference = $|V2 - V1| / (V2 + V1) * 200$
 Percent overlap = $(V1 \cap V2) / (V2 + V1) * 200$
 Where V1 is first measurement, V2 second measurement, and $V1 \cap V2$ the overlap between V1 and V2.

Reliability measures for the manual region drawing for repeat measurements on the 6 subjects are presented in Table 1, and are comparable with those of Mueller et al. [4] showing that we can obtain good depiction of the internal structure of the hippocampus at 3T. Interrater reliability was assessed by a second trained observer (EJB) performing the analysis on the 6 cases, and the results are also presented in Table 1. In order to compare the two different image protocols on the 4 of these 6 subjects who had both coronal image sequences, we repeated the segmentations using just the lower resolution image (0.4×0.5 mm) and compared these to the segmentations performed on the averaged image from all four acquisitions (lower resolution plus three higher resolution image). The comparison data are shown in the table. There is good agreement between measurements on the sequences, apart from the CA2 area.

As described above, we followed the method of Mueller et al. [4] which uses the location of the hypointense line in the hippocampus to determine the boundary between CA1 and CA2 and CA3/4 (Fig. 1). Since we observed considerable variability in how clearly this line could be visualized between subjects,

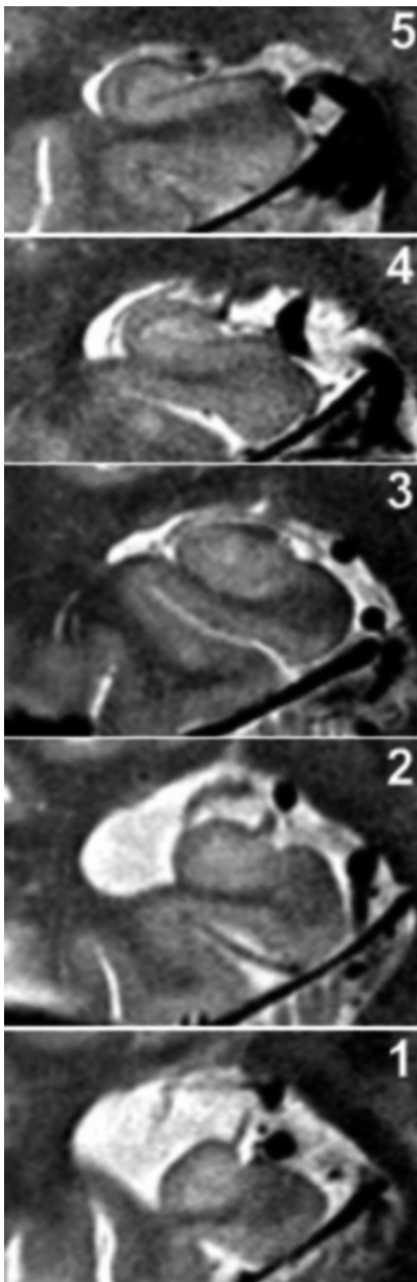


Fig. 2. Example hippocampi with visual rating for clearness. The visual rating is indicated in the top right of each hippocampus. The scale was based on the visibility of the dark line separating CA1 from CA3/4. Rating of 5 = line clearly visible on all slices; 3 = line partly visible; 1 = line not at all visible.

each hippocampus was assigned a score (1 to 5) according to how clearly the hippocampus internal structure was depicted throughout the 3 slices examined. On this scale, 5 = line clearly visualized throughout, 4 = most of the line clearly visualized, 3 = line semi

clearly defined, 2 = line mostly not clearly defined, but recognizable, 1 = line not visualized at all (see Fig. 2 for example of each category). This was done at the same time as the region of interest drawing by the same investigator, again blinded to diagnosis. Reliability of the rating scale was assessed on the same cases as the hippocampus regions, and results are also presented in Table 1.

We also obtained on all subjects a T1 weighted whole brain scan. We processed this scan to segment into grey and white matter and cerebrospinal fluid using SPM 5 (<http://www.fil.ion.ucl.ac.uk/spm/>) from which the total intracranial volume (ICV) was determined by the sum of these three components. This was then used to control for differences in head size between individuals. We also used a previously validated automated segmentation technique [26] to determine the volume of left and right hippocampi from the T1 weighted image. This procedure uses the grey matter segmentation from SPM5, along with a standard hippocampus template to segment the hippocampus. The SPM grey/white matter and hippocampus segmentations were visually checked for any gross errors.

Statistics

We tested all variables for normality using the Kolmogorov Smirnov test. All apart from education, UPDRS, and Rey scores were normally distributed. The Levene test was then used to compare homogeneity of variance and, apart from MMSE, CAMCOG and Fluctuation all had equal variances across groups. Education was dichotomized at 11 years (i.e., those who left school aged 16). Fisher's exact test was used to compare gender and post-16 education. We used ANOVA to compare normally distributed demographic factors and the Kruskal-Wallis test for the non-normally distributed variable between groups, followed by post hoc tests using Mann-Whitney, with a Bonferroni correction ($p = 0.05/3 = 0.016$) for multiple comparisons.

Since education varied between groups, it was included as a covariate in the analysis of the imaging data. Differences in hippocampal area between groups were examined with a three group ANCOVA with covariates of age, ICV, and the binary variable of post-16 education, followed by Tukey post-hoc tests. To test the discriminant power, we used discriminant analysis with cross validation (leave one out). Wilks' Lambda test was used to assess the significance of the discriminant model. We investigated the relationship between memory function (Rey delayed recall and Rey

Table 2
Subject demographics

	Control <i>N</i> = 16	AD <i>N</i> = 16	DLB <i>N</i> = 16	
Age in years	76.3 (8.2) [61-93]	77.3 (8.9) [64-94]	81.0 (5.9) [70-88]	$F = 1.6; p = 0.2$
Sex (Female :Male)	7:9	8:8	6:10	$p = 0.9$
Education in years	11.5 [9-18]	10.5 [9-16]	9.0 [8-10] ^{b,c}	$H = 18; p = 0.001$
Education post 16 (Yes:No)	8:8	5:11	0:16 ^{b,c}	$p = 0.004$
MMSE	29 [26-30]	21.5 [16-27] ^a	18 [15-27] ^c	$H = 31; p < 0.001$
Duration dementia (months)	–	40.4 (25) [6-72]	43.7 (24) [3-96]	$t = 0.16; p = 0.9$
UPDRS	2.0 [0-14]	5.5 [1-13] ^a	17.5 [9-33] ^{b,c}	$H = 32; p < 0.001$
CAMCOG	97 (3.5)	69 (11.4) ^a	67.4 (14.0) ^c	$H = 32; p < 0.001$
NPI total	–	8.5 (11.8)	24.1 (11.7) ^b	$t = 3.6; p = 0.001$
Rey total trials 1–5 (max 75)	42 [30-61]	21 [5-31] ^a	18 [4-36] ^c	$H = 31; p < 0.001$
Rey delayed recall (max 15)	8 [5-14]	0.0 [0-3] ^a	1.0 [0-8] ^{b,c}	$H = 35; p < 0.001$
Fluctuation score	0 [0] (<i>n</i> = 4)	0 [0-9]	7 [0-16] ^{b,c}	$H = 13; p = 0.002$
Hypertension Yes: No	7: 9	6: 10	6: 10	$p = 0.7$
Diabetes Yes: No	1: 15	2: 14	0: 16	$p = 0.3$
Intracranial volume (ml)	1504 (150)	1449 (159)	1472 (140)	$F = 0.56, p = 0.6$

Values in the table are mean (SD) or median [range]; Footnotes: *Post hoc* $p < 0.05$ (a) AD vs. Control; (b) DLB vs. AD; (c) DLB vs. Control; H is the Kruskal Wallis test statistic; MMSE = mini mental state exam; CAMCOG = Cambridge cognitive exam; UPDRS = Unified Parkinson's disease rating scale (subsection 3); NPI = Neuropsychiatric inventory; Rey = Rey auditory verbal learning test; Fluctuation score = Clinical Assessment of Fluctuation scale; Education post 16 and sex – Fisher's exact test; *Post Hoc* (Mann Whitney); Education: Con > DLB $p < 0.001$; AD > DLB $p = 0.001$; MMSE: Con > AD $p < 0.001$; Con > DLB $p < 0.001$; CAMCOG: Con > AD $p < 0.001$; Con > DLB $p < 0.001$; UPDRS Con < AD $p < 0.008$; Con < DLB $p < 0.001$; AD < DLB $p < 0.001$; Rey 1–5: Con > AD $p < 0.001$; Con > DLB $p < 0.001$; Rey delayed: Con > AD $p < 0.001$; Con > DLB $p < 0.001$; AD < DLB $p = 0.001$; Fluctuation: Con > DLB $p = 0.01$; AD > DLB $p = 0.006$.

total item score) and those hippocampus measurements which showed a group difference using a Spearman correlation within each group separately. All p values quoted are two sided. Results were regarded as significant if $p < 0.05$. All statistical analysis was performed with Minitab 15 (Minitab Inc., Pennsylvania, USA).

RESULTS

Subject and image characteristics

Demographic data is summarized in Table 2. There were no difference between groups in age or sex, presence of hypertension, or diabetes, but the DLB subjects had fewer years of education than both control and AD subjects. Intracranial volumes did not differ between groups and there was no difference between AD and DLB groups in MMSE, CAMCOG, or duration of dementia. As would be expected, the UPDRS and NPI scores were higher in DLB subjects as was the Rey delayed recall score, the latter indicative of better preserved memory function that is characteristic of DLB subjects.

Images were generally of good quality, with only one high resolution MR (from a DLB subject) not usable due to motion. However, early on in the study, we noticed that in those subjects with atrophied hippocampi,

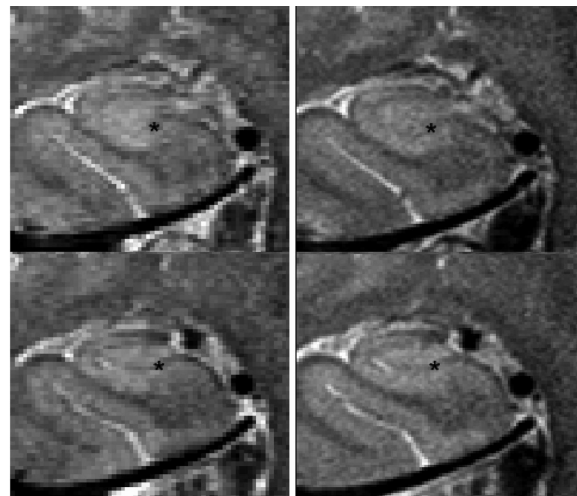


Fig. 3. Left column – hippocampus imaging in first 13 subjects (with resolution of 0.41×0.52 mm), right column – imaging used in subsequent subjects, with higher image resolution (0.27×0.35 mm). Note the hypointense line (indicated by an asterisk) in the hippocampus is more clearly depicted in the higher resolution image, allowing better definition of the subfield boundaries.

the hypointense band which divides CA1 from CA3/4 was not consistently visible. To try to improve visibility of substructures, after the first 13 subjects (5 Control, 7 AD, 1 DLB), we added a sequence with increased coronal resolution (from 24 coronal slices with resolu-

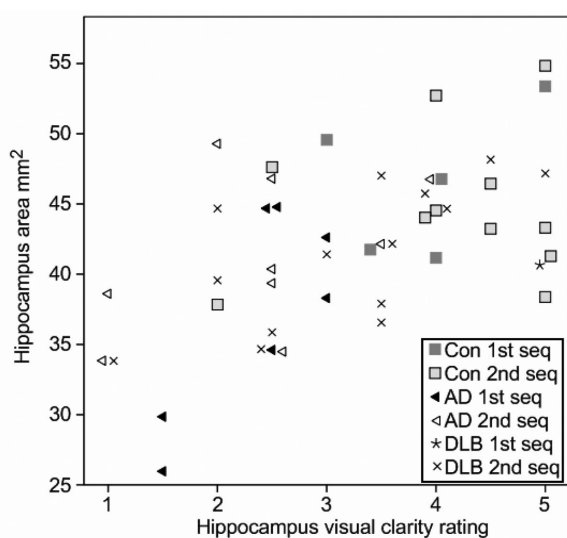


Fig. 4. Graph of average of left and right hippocampus visual clarity rating vs average hippocampus area. Data acquired with the two different T2 weighted imaging protocols are shown (1st seq – resolution of 0.41×0.52 mm; 2nd seq – resolution of 0.27×0.35 mm).

tion 0.4×0.5 to 12 slices with 0.27×0.35 resolution; see Fig. 3 for a comparison in a normal subject). There were no significant differences ($p > 0.2$) in any hippocampal measurements between images from the two sequences in any group.

Hippocampus measurements

Table 3 summarises the hippocampal measurements on the three groups in the 6mm thick anterior portion of the hippocampus body that we examined. Controlling for age, ICV, and post-16 education, we found the subiculum thickness was significantly reduced in AD compared to both control and DLB ($p < 0.01$). The area of CA1 was also reduced in AD relative to both control and DLB. Entorhinal cortex thickness was reduced in AD compared to controls, with DLB not being significantly different to either group. There was, however, no difference between any of the groups in CA2 or CA3/4. Table 3 also shows values from the automated segmentation of the whole hippocampus from the T1 weighted image. Both the AD and DLB groups had significantly smaller hippocampi than the control group, and there was no difference between AD and DLB in hippocampal volume.

Visual rating

As mentioned above, we noticed that the definition of the hippocampus subregions was less clear in some

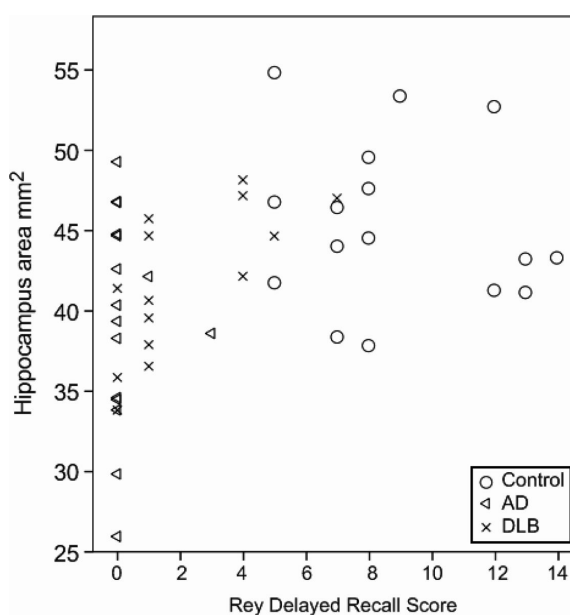


Fig. 5. Graph of average hippocampus area vs. Rey delayed memory score in the three groups.

scans, suggesting structural changes potentially relating to the underlying disease process. We therefore visually rated the clearness of the scan on a 1–5 scale for the three slices on which the hippocampus regions were drawn. Typical scan data illustrating hippocampi with each of the 5 scores are shown in Fig. 2. Figure 4 shows the relationship to hippocampal size and diagnostic group. In a general linear model, predictors of the visual rating were diagnosis ($F = 7.7$; $p = 0.002$), hippocampus area ($F = 11.9$; $p = 0.001$), but not intracranial volume ($p = 0.4$) or imaging sequence (0.4×0.5 mm versus 0.27×0.35 mm: $F = 2.8$; $p = 0.1$).

Removing the 3 subjects (2 AD, 1 DLB) with the worst hippocampus clearness rating did not alter the significance of any of the findings.

Predictive diagnostic ability

To investigate the potential discriminating power of the hippocampal measurement, we performed a linear regression to find the best predictors, with group (AD versus DLB) as the dependent variable, age, ICV, and education as fixed covariates, and all of the hippocampal measurements added to the model in a step-wise fashion. This produced a model ($F = 12.3$; $p < 0.001$) in which subiculum thickness ($p = 0.005$), visual clearness ($p = 0.001$), and hippocampus volume ($p = 0.024$) independently predicted group member-

Table 3

Comparison of hippocampal measurements in the three groups. Values quoted are the average of the left and right side measurements made on three adjacent image slices. The hippocampus volume is from automated segmentation of the T1 weighted MPRAGE sequence. ANCOVA differences between AD/control/ DLB controlling for age, intracranial volume and post 16 education. All values are mean (SD) [95% Confidence interval]

	Control	AD	DLB	ANCOVA F; p
CA1 area mm ²	26.7 (3.1) [25-28]	22.6 (3.9) [21-25] ^{a,b}	23.8 (3.0) [22-25]	$F = 6.3; p = 0.004$
CA2 area mm ²	1.53 (0.31) [1.36-1.70]	1.45 (0.33) [1.27-1.62]	1.53 (0.38) [1.33-1.75]	$F = 0.1; p = 0.9$
CA2 thickness mm	1.36 (0.15) [1.28-1.43]	1.30 (0.19) [1.20-1.40]	1.32 (0.19) [1.21-1.42]	$F = 0.3; p = 0.7$
CA3/4 area mm ²	17.2 (2.2) [16.1-18.4]	15.5 (3.0) [13.9-17.1]	16.0 (2.4) [14.7-17.3]	$F = 1.4; p = 0.3$
Entorhinal thickness mm	2.25 (0.18) [2.16-2.35]	1.87 (0.24) [1.74-2.00] ^a	1.96 (0.27) [1.81-2.11]	$F = 9.9; p < 0.001$
Subiculum thickness mm	2.37 (0.28) [2.22-2.52]	2.03 (0.29) [1.87-2.18] ^{a,b}	2.35 (0.24) [2.22-2.48]	$F = 9.1; p = 0.001$
Hippocampus area mm ²	45.4 (5.2) [43-48]	39.5 (6.5) [36-43] ^a	41.3 (4.8) [39-44]	$F = 4.2; p = 0.022$
Subfield visual clarity	4.0 (0.9) [3.6-4.6]	2.4 (0.8) [1.9-2.8] ^{a,b}	3.3 (1.1) [2.7-3.9]	$F = 16; p < 0.001$
Hippocampus volume mm ³	2878 (333) [2700-3055]	2163 (551) [1870-2457] ^a	2078 (616) [1737-2419] ^c	$F = 8.6; p = 0.001$

Post hoc $p < 0.05$ (a) AD vs. Control; (b) AD vs. DLB; (c) DLB vs. Control; *Post hoc* comparisons (Tukey); CA1 area: Control > AD $p = 0.007$; AD < DLB $p = 0.043$; Subiculum thickness: Control > AD $p = 0.006$; AD < DLB $p = 0.002$; Entorhinal thickness: Control > AD $p < 0.001$; Hippocampus area: Control > AD $p = 0.03$; Subfield clarity: Control > AD $p < 0.001$; AD < DLB $p < 0.001$; Hippocampus volume: Control > AD $p < 0.001$; Control > DLB $p = 0.01$.

ship. We then performed discriminant analysis with cross validation to estimate discriminating power with subiculum, clearness, and hippocampal volume to classify group (AD versus DLB). This correctly classified 81% (14 AD and 11 DLB; $p = 0.007$). Hippocampal volume by itself did not classify subjects above chance (61% correct; $p = 0.7$), while using just subiculum and clearness correctly classified 74% of subjects (11 AD and 12 DLB; $p = 0.005$), and either variable by itself performed almost as well: clearness 71% (12 AD & 10 DLB; $p = 0.015$) subiculum 71% (9 AD & 13 DLB; $p = 0.002$).

Memory function

To see if the hippocampus measurements related to memory function, we performed a Spearman correlation in each group of CA1, subiculum, entorhinal cortex, hippocampal area, hippocampus volume (from automated segmentation), and visual clearness against Rey delayed recall and Rey total items. In the DLB group, there were significant correlations between Rey delayed score and hippocampus area ($r = 0.7$; $p = 0.004$), hippocampus volume ($r = 0.8$; $p < 0.001$), CA1 area ($r = 0.7$; $p = 0.011$), and visual clearness ($r = 0.6$ $p = 0.03$). There were no significant correlations in the AD or control group. Figure 5 shows the Rey delayed memory score plotted against average hippocampus area. As Fig. 5 shows, the lack of correlation in the AD group is due to floor effects in the memory test for that group.

Slice angulation

We had oriented the coronal images via the corpus

collosum. To verify how perpendicular the image slices were to the hippocampus at the point of measurement, we calculated the centre of the manually drawn hippocampus regions on each of the three slices. From the shift in the up-down position of the ROI centre, we estimated the angulation of the hippocampus relative to the image perpendicular. For the left hippocampus, Control 11.3 ± 8.4 (mean \pm SD); AD 7.0 ± 8.6 ; DLB 2.8 ± 8 degrees, and for right, Control 10.6 ± 7.0 ; AD 8.1 ± 6.0 ; DLB 3.4 ± 7.9 degrees. There were no significant differences between left and right hippocampus in any group. A group comparison ANOVA found $F = 3.5$, $p = 0.038$ in left side and $F = 4.2$, $p = 0.022$ on the right with a *post hoc* difference ($p = 0.02$) of about 7 degrees between the control and DLB group, but no other significant differences between groups.

DISCUSSION

The main finding of the study was that on high field strength hippocampal MR imaging, in DLB, the subiculum, and CA1 areas in the anterior portion of the hippocampus body were significantly less atrophied than in AD. The entorhinal cortex was smaller in AD, with DLB being intermediate between control and AD, while there was no difference in the CA2 and CA3/4 regions. These data add to previous studies in AD and DLB which assessed overall hippocampal atrophy [6–8] and further support the hypothesis that the medial temporal lobe is differentially affected in the two dementias.

Adachi, using high resolution coronal diffusion imaging of the hippocampus, also observed CA1 and

subiculum atrophy in AD, with no CA3/4 atrophy compared to control subjects [27]. Using a comparable coronal sequence to the one in this study at 4T, Mueller et al. [5] found CA1, CA2, entorhinal cortex, and subiculum reduced in AD compared with controls, while the CA3/4 area was only reduced in those with the apolipoprotein E (ApoE) $\epsilon 4$ allele. Burggren [25], in (asymptomatic) ApoE $\epsilon 4$ carriers using a similar imaging sequence, found only differences in entorhinal cortex and subiculum, not CA1, CA2, or CA3/4. They also found that thickness measurements were more reliable than area. We did not have information on ApoE $\epsilon 4$ status of our subjects, and hence could not investigate its relationship to hippocampus atrophy.

The majority of studies using T1 weighted imaging and subregions inferred from the hippocampus surface have also found CA1 and subiculum, but not CA2 or CA3/4 atrophy relative to controls. [1,2,28] The study of Sabattoli [9] with such a 1 mm³ resolution T1 weighted sequence, found atrophy in DLB versus AD mostly confined to the head of the hippocampus, whereas the regions of greater atrophy in AD were largely in the tail, but also CA1 and subiculum of the hippocampal body.

It is possible that our lack of significant difference in CA2 was due to the increased variability in measuring this structure, due to its small size, and difficulty discerning its boundaries within the hippocampus. However, in an attempt to increase reliability, we measured both area and thickness of the structure, and in neither case was there any indication of a significant difference between the groups. The high variability of the CA2 region both between raters, and within rater on the two different sequences used does limit the interpretation of our finding of no difference in CA2 between groups. Unfortunately, we did not discover any means of reliably identifying CA2 medial and lateral borders. The entorhinal cortex measurement also had greater intra-rater variability, which may have made it more difficult to find differences between DLB and AD or control groups. We used the thickness rather than area of the subiculum and entorhinal cortex rather than area due to large variations in the length of these structures. Although this gave a more precise measurement, it does mean that we were not sensitive to changes in the overall shapes.

The CA1 region was differentiated from the CA3/4 region by determining the location of a hypointense line on the image. This line is likely to represent fibers in the hippocampal layers of stratum moleculare, stratum lacunosum, and stratum radiatum [29,30]. We found

that the visibility of this line in the anterior portion of the hippocampus body varied considerably between cases, and was less clear in AD subjects and those with smaller hippocampi. This variable visibility either represents changes in the MR relaxation properties of these layers, or loss of the underlying tissue itself. In either case it potentially represents disease related changes in the internal structure of the hippocampus. A study by Kantarci [31] used diffusion weighted imaging and found that increased diffusivity in the hippocampus of MCI subjects predicted conversion to AD, indicating early loss or damage to neuronal bodies in the hippocampus. Hippocampal atrophy has been found to relate to changes in WM of the cingulum which connects the hippocampus to the posterior cingulate [32, 33], suggesting that breakdown of the white matter in and connecting the hippocampus is associated with atrophy, a notion supported by our findings.

We saw correlations in the DLB group between memory function and CA1 and overall hippocampus area, suggesting that hippocampal atrophy (possibly due to concomitant AD pathology) is related to worsening short term memory, as would be expected. We did not see any correlations in the AD group, probably due to floor effects; the maximum score on the Rey delayed test was 3/15 in the AD group (Fig. 5). Due to the relatively small numbers in each group, these results should be considered tentative.

We found reasonable predictive ability of the subiculum thickness to distinguish AD from DLB, with 71% of cases correctly classified. In this study, it was better than any other hippocampal measurement, including overall area or volume. In the revised international consensus criteria for clinical diagnosis of DLB [15], a visual rating of overall hippocampal atrophy can be used as a supportive feature for diagnosis. Possibly subiculum thickness could provide additional diagnostic information and further studies on larger numbers of subjects should investigate whether subiculum thickness provides a more specific diagnostic discriminator. This is important, as another putative specific marker for AD, atrophy of the entorhinal cortex, did not differentiate between AD and DLB, similar to findings from a previous study using more standard 1.5T imaging [10]. Previous studies have found similar levels for discriminating AD from DLB on hippocampus volume. Data from Whitwell et al. [7] suggest a diagnostic accuracy of 65%, while Barber et al. [34] had an accuracy of 74% for DLB versus AD. However in our study, the hippocampus area and volume by themselves did not distinguish between AD and DLB, suggesting that the

subiculum and visual rating might provide additional diagnostic information that is complementary to measurement of overall hippocampus atrophy. Scans using the dopamine transporter tracer FPCIT have been shown in a large multicenter study to have a very good (85%) accuracy for distinguishing DLB from non-DLB dementia [35]. However, MRI has the advantage that information can also be acquired in the same scanning session about other pathologies (i.e., vascular).

Strengths of the study include high resolution hippocampus imaging and careful ROI measurements. The cohort was well defined, with all dementia subjects fulfilling criteria for either probable AD or probable DLB, using a clinical diagnostic method we have previously validated against postmortem findings and utilizing dopaminergic imaging in 9 DLB subjects. Weaknesses are that only a 6 mm portion of the hippocampus body was examined, and (as noted by Mueller et al. [5]) the boundaries of CA2 are somewhat arbitrary. We used two different imaging protocols, as we tried to improve the image resolution during the study, and the initial 13 subjects were not rescanned. Although this is a potential confounder, we obtained good agreement between the area and thickness measurements made on the two sequences, and controlling for the type of sequence used in the analysis did not alter the results. Detection of hippocampal substructures requires sufficient in-plane resolution and image contrast between individual structures. Although our sequences were based largely on the study of Mueller et al. [4] which was performed at higher field (4 Tesla), we conducted preliminary investigations varying sequence parameters (TR and TE) and did not obtain any significant improvement in contrast.

We positioned the coronal scans in this study relative to the corpus callosum, rather than angling them according to the hippocampus. This has the advantage of being an easy method to reproduce in clinical practice, rather than the difficult task of determining a plane perpendicular to both hippocampi (whose axis varies medio-laterally and between left and right). However, it also means that the image plane was not strictly perpendicular to the hippocampi, which will cause small errors in distance measurement varying with the cosine of the angle. We measured the angulation of the hippocampus from the manually drawn regions, and found good alignment, with an 11 degree difference between image perpendicular and hippocampus axis in the control group. The variability in the area/distance measurement will be governed by the SD of the angulation which was 7–10 degrees. For a 10 degree difference

between the image plane perpendicular and hippocampus axis, there will be a 1.5% difference in distance measurement. This is much smaller than the SD in all measurements (Table 3) and suggests that variation in alignment is a minor source of error in the study.

An important limitation of the study was that the measurement of subiculum and entorhinal cortex was not validated by an established technique. Following Mueller et al., our working definition for the medial boundary of CA1 was to use the superficial hippocampal sulcus. While this is a consistent and easily identified boundary, it does mean that the CA1 region will include some of the subiculum, and hence our CA1 findings will be slightly influenced by any subiculum changes.

We did not have autopsy confirmation of the diagnoses in the subjects, however we used a consensus clinical diagnosis, which we have previously shown to have good accuracy against autopsy [16]. In addition, all 9 of our DLB subjects who had dopamine transporter imaging had abnormal scans consistent with DLB as the diagnosis. It is quite possible that the DLB subjects had some degree of concomitant AD pathology, which contributed to the hippocampus atrophy. A CT image was used as part of the clinical diagnosis, and this does have the potential to bias the sample towards AD having greater hippocampal atrophy. We do not feel this was a major issue, since the hippocampus volume did not differ between the AD and DLB groups. For the hippocampus volume measurement, we used an automated technique. This is not as accurate as the gold standard of manually tracing (though much quicker) and may give incorrect results in subjects with abnormalities/severe atrophy. However, we have previously shown good reliability with this method in a dementia population [26] and feel the results should be representative.

Our data were collected close to the current limit of in-plane spatial resolution achievable at 3 Tesla and as a result have relatively low signal to noise. Further improvements in resolution could be made at the expense of much longer data collection times, but these are likely to be inappropriate in these patient groups and suffer from image degradation due to subject movement. Ultra-high field strength MRI (7 Tesla and above) can offer significant improvements in resolution (between than 0.5 mm isotropic resolution) and, provided subject movement can be minimized, will provide opportunities to further investigate the changes in substructures which we have observed.

The fact that we observed less clear definition of hippocampal structures in AD was interesting in that it in-

licated internal breakdown of the hippocampus. However, it also will have limited the accuracy of delimiting the subregions. Moreover, the analysis did not change on excluding those with the least clear hippocampi. The subiculum thickness measurement was relatively clear on all subjects as its upper surface was the ventricle, and lower surface, the temporal lobe white matter, and it showed good intra-rater reliability (ICC was 0.8). If replicated in a larger study, the subiculum thickness could be a simply measured useful additional diagnostic feature of AD versus DLB.

ACKNOWLEDGMENTS

We are grateful for funding from the Alzheimer's Research Trust. This work was supported by the UK NIHR Biomedical Research Centre for Ageing and Age-related disease award to the Newcastle upon Tyne Hospitals NHS Foundation Trust. We also thank the North East DeNDRoN (Dementia and Neurodegenerative Diseases Research Network) team for help with subject recruitment, and Philip English for useful discussions on MR sequence parameters.

Authors' disclosures available online (<http://www.jalz.com/disclosures/view.php?id=455>).

REFERENCES

- [1] Chételat G, Fouquet M, Kalpouzos G, Denghien I, De la Sayette V, Viader F, Mézenge F, Landeau B, Baron JC, Eustache F, Desgranges B (2008) Three dimensional surface mapping of hippocampal atrophy progression from MCI to AD and over normal aging as assessed using voxel-based morphometry. *Neuropsychologia* **46**, 1721-1731.
- [2] Frisoni GB, Sabattoli F, Lee AD, Dutton RA, Toga AW, Thompson PM (2006) In vivo neuropathology of the hippocampal formation in AD: A radial mapping MR-based study. *NeuroImage* **32**, 104-110.
- [3] Rössler MZ, R. Bohl, J. Ohm, T.G. (2002) Stage-dependent and sector-specific neuronal loss in hippocampus during Alzheimer's disease. *Acta Neuropathologica* **103**, 363-369.
- [4] Mueller SG, Stables L, Du AT, Schuff N, Truran D, Cashdollar N, Weiner MW (2007) Measurement of hippocampal subfields and age-related changes with high resolution MRI at 4T. *Neurobiol Aging* **28**, 719-726.
- [5] Mueller SG, Schuff N, Raptentsetsang S, Elman J, Weiner MW (2008) Selective effect of Apo e4 on CA3 and dentate in normal aging and Alzheimer's disease using high resolution MRI at 4T. *NeuroImage* **42**, 42-48.
- [6] Tam CW, Burton EJ, McKeith IG, Burn DJ, O'Brien JT (2005) Temporal lobe atrophy on MRI in Parkinson disease with dementia: a comparison with Alzheimer disease and dementia with Lewy bodies. *Neurology* **64**, 861-865.
- [7] Whitwell JL, Weigand SD, Shiung MM, Boeve BF, Ferman TJ, Smith GE, Knopman DS, Petersen RC, Benarroch EE, Josephs KA, Jack CR (2007) Focal atrophy in dementia with Lewy bodies on MRI: a distinct pattern from Alzheimer's disease. *Brain* **130**, 708-719.
- [8] Barber R, Gholkar A, Scheltens P, Ballard C, McKeith IG, O'Brien JT (1999) Medial temporal lobe atrophy on MRI in dementia with Lewy bodies. *Neurology* **52**, 1153-1158.
- [9] Sabattoli F, Boccardi M, Galluzzi S, Treves A, Thompson PM, Frisoni GB (2008) Hippocampal shape differences in dementia with Lewy bodies. *NeuroImage* **41**, 699-705.
- [10] Kenny ER, Burton EJ, O'Brien JT (2008) A volumetric magnetic resonance imaging study of entorhinal cortex volume in dementia with Lewy bodies. *Dement Geriatr Cogn Disord* **26**, 218-225.
- [11] Iseki E, Takayama N, Marui W, Ueda K, Kosaka K (2002) Relationship in the formation process between neurofibrillary tangles and Lewy bodies in the hippocampus of dementia with Lewy bodies brains. *J Neurol Sci* **195**, 85-91.
- [12] Dickson DW, Ruan D, Crystal H, Mark MH, Davies P, Kress Y, Yen SH (1991) Hippocampal degeneration differentiates diffuse Lewy body disease (DLBD) from Alzheimer's disease - light and electron microscopic immunocytochemistry of CA2-3 neurites specific to DLBD. *Neurology* **41**, 1402-1409.
- [13] Harding AJ, Lakay B, Halliday GM (2002) Selective hippocampal neuron loss in dementia with Lewy bodies. *Ann Neurol* **51**, 125-128.
- [14] McKhann G, Drachman D, Folstein M, Katzman R, Price D, Stadlan EM (1984) Clinical diagnosis of Alzheimer's disease: Report of the NINCDS-ADRDA Work Group under the auspices of Department of Health and Human Services Task Force on Alzheimer's disease. *Neurology* **34**, 939-944.
- [15] McKeith IG, Dickson DW, Lowe J, Emre M, O'Brien JT, Feldman H, Cummings J, Duda JE, Lippa C, Perry EK, Aarsland D, Arai H, Ballard CG, Boeve B, Burn DJ, Costa D, Del Ser T, Dubois B, Galasko D, Gauthier S, Goetz CG, Gomez-Tortosa E, Halliday G, Hansen LA, Hardy J, Iwatsubo T, Kalaria RN, Kaufer D, Kenny RA, Korczyn A, Kosaka K, Lee VM-Y, Lees A, Litvan I, Londo E, Lopez OL, Minoshima S, Mizuno Y, Molina JA, Mukaetova-Ladinska EB, Pasquier F, Perry RH, Schulz JB, Trojanowski JQ, Yamada M (2005) Diagnosis and management of dementia with Lewy bodies: Third report of the DLB consortium. *Neurology* **65**, 1863-1872.
- [16] McKeith IG, Ballard CG, Perry RH, Ince PG, O'Brien JT, Neill D, Lowery K, Jaros E, Barber R, Thompson P, Swann A, Fairbairn AF, Perry EK (2000) Prospective validation of Consensus criteria for the diagnosis of dementia with Lewy bodies. *Neurology* **54**, 1050-1058.
- [17] Roth M, Tym E, Mountjoy CQ, Huppert FA, Hendrie H, Verma S, Goddard R (1986) CAMDEX - A Standardised instrument for the diagnosis of mental disorder in the elderly with special reference to the early detection of dementia. *Br J Psychiatry* **149**, 698-709.
- [18] Alexopoulos GS, Abrams RC, Young RC, Shamoian CA (1988) Cornell scale for depression in dementia. *Biol Psychiatry* **23**, 271-284.
- [19] Cummings JL, Mega M, Gray K, Rosenberg-Thompson S, Carusi DA, Gornbein J (1994) The neuropsychiatric inventory: comprehensive assessment of psychopathology in dementia. *Neurology* **44**, 2308-2314.
- [20] Walker MP, Ayre GA, Cummings JL, Wesnes K, McKeith IG, O'Brien JT, Ballard CG (2000) The clinician assessment of fluctuation and the one day fluctuation assessment scale. *Br J Psychiatry* **177**, 252-256.

- [21] Rey A (1964) *L'examen Clinique en Psychologie*. Presses Universitaires de France, Paris.
- [22] Fahn S, Elton R, Members of the UPDRS development committee (1987) Unified Parkinson's disease rating scale In *Recent developments in Parkinson's disease*, Fahn S, Marsden CD, Calne DB, Goldstein M, eds. MacMillan Healthcare Information, Florham Park; NJ.
- [23] Jenkinson M, Smith SM (2001) A global optimisation method for robust affine registration of brain images. *Medical Image Analysis* **5**, 143-156.
- [24] Yushkevich PA, Piven J, Hazlett HC, Smith RG, Ho S, Gee JC, Gerig G (2006) User-guided 3D active contour segmentation of anatomical structures: significantly improved efficiency and reliability. *NeuroImage* **31**, 1116-1128.
- [25] Burggren AC, Zeineh MM, Ekstrom AD, Braskie MN, Thompson PM, Small GW, Bookheimer SY (2008) Reduced cortical thickness in hippocampal subregions among cognitively normal apolipoprotein E e4 carriers. *NeuroImage* **41**, 1177-1183.
- [26] Firbank MJ, Barber R, Burton EJ, O'Brien JT (2008) Validation of a fully automated hippocampal segmentation method on patients with dementia. *Human Brain Mapping* **29**, 1442-1449.
- [27] Adachi M, Kawakatsu S, Hosoya T, Otani K, Honma T, Shibata A, Sugai Y (2003) Morphology of the inner structure of the hippocampal formation in Alzheimer disease. *Am J Neuroradiol* **24**, 1575-1581.
- [28] Wang L, Miller JP, Gado MH, McKeel DW, Rothermich M, Miller MI, Morris JC, Csernansky JG (2006) Abnormalities of hippocampal surface structure in very mild dementia of the Alzheimer type. *NeuroImage* **30**, 52-60.
- [29] Wieshmann UC, Symms MR, Mottershead JP, MacManus DG, Barker GJ, Tofts PS, Revesz T, Stevens JM, Shorvon SD (1999) Hippocampal layers on high resolution magnetic resonance images: real or imaginary? *J Anat* **195**, 131-135.
- [30] Thomas BP, Welch EB, Blake D, Niederhauser BD, Whetsell WO, Anderson AW, Gore JC, Avison MJ, Creasy JL (2008) High resolution 7T MRI of the human hippocampus in vivo. *J Magn Reson Imaging* **28**, 1266-1272.
- [31] Kantarci K, Petersen RC, Boeve BF, Knopman DS, Weigand SD, O'Brien PC, Shiung MM, Smith GE, Ivnik RJ, Tangalos EG, Jack CR (2005) DWI predicts future progression to Alzheimer disease in amnesic mild cognitive impairment. *Neurology* **64**, 902-904.
- [32] Villain N, Desgranges B, Viader F, de la Sayette V, Mézence F, Landeau B, Baron J-C, Eustache F, Chételat G (2008) Relationship between hippocampal atrophy, white matter disruption, and gray matter hypometabolism in Alzheimer's disease. *J Neurosci* **28**, 6174-6181.
- [33] Xie S, Xiao JX, Wang YH, Wu HK, Gong GL, Jiang XX (2005) Evaluation of bilateral cingulum with tractography in patients with Alzheimer's disease. *Neuroreport* **16**, 1275-1278.
- [34] Barber R, Ballard C, McKeith IG, Gholkar A, O'Brien JT (2000) MRI volumetric study of dementia with Lewy bodies. *Neurology* **54**, 1304-1309.
- [35] McKeith I, O'Brien J, Walker Z, Tatsch K, Booij J, Darcourt J, Padovani A, Giubbini R, Bonuccelli U, Volterrani D, Holmes C, Kemp P, Tabet N, Meyer I, Reiningner C (2007) Sensitivity and specificity of dopamine transporter imaging with I-123-FP-CIT SPECT in dementia with Lewy bodies: a phase III, multicentre study. *Lancet Neurol* **6**, 305-313.